PROCEEDINGS OF SCIENCE

Search for a diffuse astrophysical neutrino flux with KM3NeT/ARCA using data of 2021-2022

Vasileios Tsourapis,[a,b,*] **Evangelia Drakopoulou,**[a] **Christos Markou,**[a] **Anna Sinopoulou**[c] **and Ekaterini Tzamariudaki**[a] **on behalf of the KM3NeT collaboration**

[a] *NCSR "Demokritos", Institute of Nuclear and Particle Physics, 15310 Ag. Paraskevi Attikis, Athens, Greece*

[b] *National Technical University of Athens, School of Applied Mathematical and Physical Sciences, Zografou Campus, 9, Iroon Polytechniou str, 15780 Zografou, Athens, Greece*

[c] *INFN Sezione di Catania, Via Santa Sofia,64 - 95123 Catania, Italy*

E-mail: tsourapis@inp.demokritos.gr

KM3NeT is a research infrastructure hosting two neutrino detectors which are currently under construction in the Mediterranean Sea. The KM3NeT/ARCA detector focuses on the detection of high energy neutrinos (>TeV) from astrophysical sources. In this contribution, an analysis of the data obtained during 2021-2022, using machine learning techniques, is presented. The potential of KM3NeT/ARCA to detect a diffuse flux of astrophysical neutrinos at the early stages of the detector construction is reported. The results of this analysis are presented.

38th International Cosmic Ray Conference (ICRC2023)
26 July - 3 August, 2023
Nagoya, Japan

*Speaker

PoS(ICRC2023)1195

1. Introduction

One of the main goals of modern astronomy is to resolve the particle acceleration mechanisms at place at distant astrophysical sources. The measurement of a diffuse flux of cosmic neutrinos can provide an insight to this endeavor. Responsible for the diffuse astrophysical neutrino flux observed at Earth are: a) the high energy cosmic rays which produce neutrinos through pp and $p\gamma$ interactions while traveling at cosmic distances and b) the collection of emitters that can not be detected individually.

At source, the ratio of the neutrino flavours is typically assumed to be $\nu_e : \nu_\mu : \nu_\tau = 1 : 2 : 0$. The probability of a certain flavour α oscillating to a different flavour β depends on the distance traveled (L) and the neutrino energy (E): $P_{\alpha\to\beta} \sim L/E$. Neutrinos traveling over cosmic distances are expected to reach the Earth with a ratio $\nu_e : \nu_\mu : \nu_\tau = 1 : 1 : 1$. The energy spectrum of these neutrinos is typically modeled as a power-law, $\Phi = \Phi_0 E^{-\gamma}$. In this work, the following parametrization is assumed:

$$\Phi_{\nu+\bar{\nu}}(E) = \frac{dN}{dE} = \phi_0 \cdot 10^{-18} \cdot \left(\frac{E}{100\ \text{TeV}}\right)^{-\gamma} \left[\text{GeV}^{-1}\text{cm}^{-2}\text{s}^{-1}\text{sr}^{-1}\right] \quad (1)$$

2. Detection method

2.1 KM3NeT detector

The KM3NeT [1] infrastructure currently hosts two Cherenkov neutrino detectors under construction in the Mediterranean Sea: KM3NeT/ARCA, offshore Capo Passero (Italy) and KM3NeT/ORCA, offshore Toulon (France). KM3NeT/ORCA is designed for studying atmospheric neutrino oscillations, while KM3NeT/ARCA is optimized for detecting neutrinos of astrophysical origin.

ARCA is located at a depth of 3500 m and, when complete, will consist of 2 Building Blocks of 115 Detection Units (DUs) each. Every DU is a vertical, string-like, structure anchored to the seabed and carrying 18 Digital Optical Modules (DOMs). A DOM [2] is the main detector element, housing 31 3"-PMTs (photo-multiplier tubes). DOMs are spaced by 36 m along a DU, with an horizontal spacing between DUs of 90m. Both ORCA and ARCA share the same design, only differing in the spacing between DUs (20 m for ORCA) and DOMs along a DU (9 m for ORCA), since the two detectors are optimised for the detection of neutrinos of different energy ranges.

Currently, the ARCA detector consists of 21 DUs and the ORCA detector of 18 DUs.

2.2 Data taking periods

Data taking periods refer to the number of deployed DUs at running time. A stable data taking period starts after the new DUs are commissioned and calibrated. In this study, the full data sample of the ARCA6/ARCA8 running periods is analyzed. ARCA6 ran from May 2021 through September 2021 for a total of 102 analyzed days and ARCA8 from September 2021 through June 2022 for a total of 212 analyzed days. The analysis has been then extended for the recent detector configurations, ARCA19 (July 2022 - September 2022) [51 analyzed days] and ARCA21 (September

2022 – December 2022) [1] [67 analyzed days] and the final results are presented. The event selection for those two periods is described in Section 5.

3. Event selection

A collection of photons that impinge on PMTs (hits) that occur within a certain distance and a specific time window, constitute an event. The underwater environment produces noise hits to the PMTs, mainly through ^{40}K decays and bioluminescence. These contributions can easily be eliminated by applying appropriate constraints on the reconstruction variables. Signal events come from neutrinos and anti-neutrinos of astrophysical origin of all 3 flavours and both interaction channels (CC and NC) reconstructed as tracks. Atmospheric (anti)neutrinos and muons represent the physics background.

3.1 Preselection

Extensive data-MC comparisons have been performed to evaluate the description of the detector performance. Several reconstruction variables are used during the preselection in order to remove the contribution of noise, as well as of events with a poor reconstruction performance, based on the previous analysis on the diffuse astrophysical neutrino flux [3]. Constraints are applied on the basis of the goodness of fit of the event reconstruction, the length of the track in the detector volume, the angular error estimate from the event reconstruction, the number of triggered DOMs, and the value of the energy estimate of the event.

Upgoing events, with zenith $> 90^o$, are selected, in order to suppress the background from atmospheric muons since only (anti)neutrinos can survive passing through the Earth.

3.2 Usage of a Boosted Decision Tree

A Boosted Decision Tree (BDT) classifier, using ROOT TMVA [4], was developed, based on the previous diffuse analysis [3], in order to better reject the atmospheric muon background. Since only upgoing events are selected, all remaining atmospheric muons are wrongly-reconstructed events.

The BDT is trained using as *class 0* well reconstructed (WR) $\overset{(-)}{\nu}_{\mu}$ CC interactions (the dominant track-like channel) and as *class 1* badly reconstructed (BR) muons; this definition relies on the amplitude of the angular difference, $\Delta\Omega$, between the neutrino direction from Monte Carlo (MC) simulations and the reconstructed track.

The model was trained using a combination of a special MC production dedicated for machine learning and a 10% of the standard MC production of the ARCA8 dataset. The rest of the MC was used for the evaluation. As input to the BDT, 15 variables extracted from the output of the event reconstruction were used, as the ones with the best separation power and smallest correlation with each other. Using the Grid Search technique, the best combination of hyper-parameters for the BDT was selected. After thorough tests, the classifier was deemed suitable to be applied also to the ARCA6 dataset.

[1] ARCA21 detector configuration is expected to complete its uptime on September 2023, when new detection units will be added. The dates here refer to the time period analyzed in this contribution.

A **blind policy** has been followed, in order to avoid any biases, according to which all cuts are optimized only on the MC and 10% of the data.

The performance of the classifier can be seen in Figure 1. For atmospheric (anti)neutrinos the Honda [5] and Enberg [6] models were used, once a correction for the presence of the cosmic ray knee was applied. For all the optimizations, the cosmic neutrino flux used, following the normalization of eq. 1, is the one presented by IceCube [7] with $\phi_0 = 1.44$ and spectral index $\gamma = 2.37$.

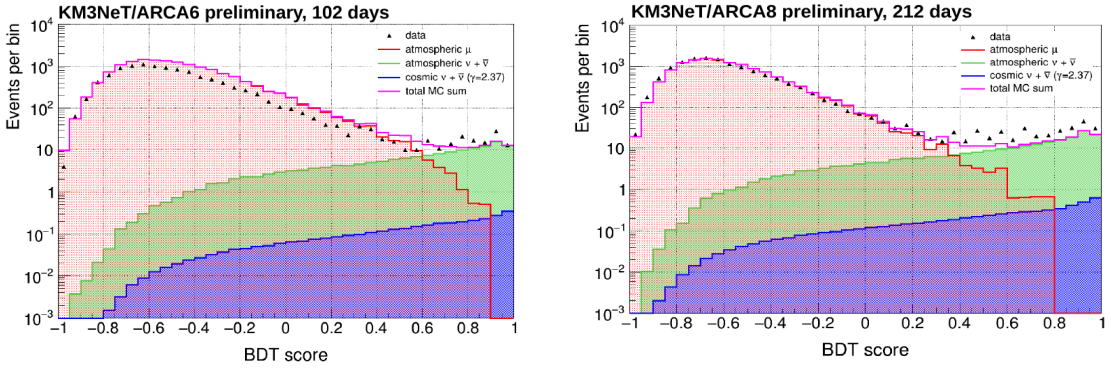

Figure 1: The BDT score distribution for all events for the ARCA6 and ARCA8 periods. 100% of the data is shown in this Figure.

The choice of the optimal BDT score cut was made after *evaluating* on a 3-flavour signal, based on the requirement that an efficiency more than 70% is reached, and that the Model Rejection Factor (MRF) is optimised [8]. The MRF procedure, based on the Feldman-Cousins [9] upper limit estimations, is also used to select the optimal energy cut value that selects the cosmic signal.

In order to account for the low statistics of the atmospheric muon MC simulation for high BDT scores and high muon energies, the atmospheric muon contribution is extracted by fitting the estimated energy spectrum *after* the BDT score selection. Also, *after* the BDT selection, the atmospheric muon contributions were scaled up by 40% to compensate for the data-MC differences. Consequently, a systematic error of 40% was assigned as referenced in Section 4.2.

The energy resolution for events surviving the BDT score cut is shown in Figure 2.

3.3 Final sample

The BDT score for ARCA6 dataset was required to be more than 0.35 and for ARCA8 more than 0.27. The optimal threshold on the logarithm of the energy estimate is 4.20 and 4.04 for ARCA6 and ARCA8, respectively.

The number of the events surviving the final selection for each category, after *unblinding*, is shown in Table 1 and the corresponding energy distributions in Figure 3.

4. Analysis method

4.1 Binned-Likelihood method

Data are analyzed using a binned-likelihood method, described in [10]. Based on the Bayesian interpretation of probability, the possibility of a certain hypothesis to be true, given some experi-

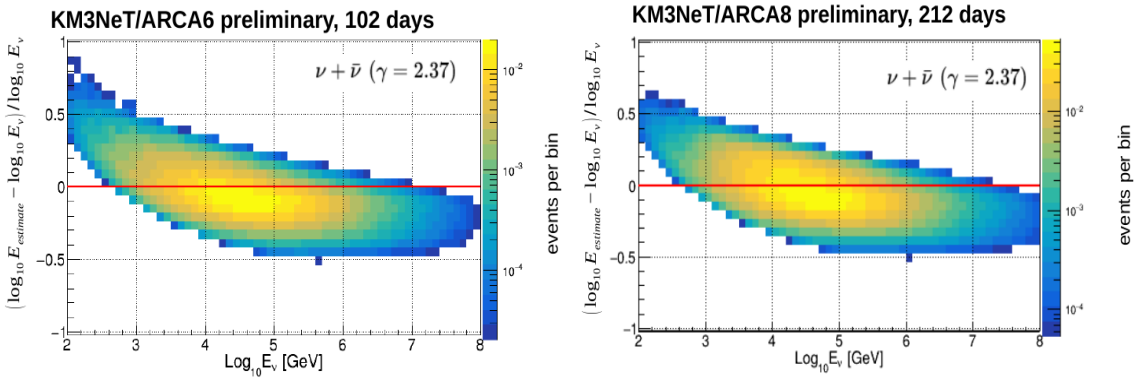

Figure 2: Energy resolution for cosmic neutrinos, after the BDT score cut is applied for ARCA6 (score > 0.35) and ARCA8 (score > 0.27), versus the true (MC) neutrino energy.

	ARCA6		ARCA8	
	BDT score > 0.35	$\log E_{estimate} > 4.20$ GeV	BDT score > 0.27	$\log E_{estimate} > 4.04$ GeV
atm. $\nu + \bar{\nu}$	117.68	16.08	185.18	33.04
atm. μ	150.91	39.07	49.12	25.39
all atmospheric	268.59	55.15	234.30	58.43
cosmic $\nu + \bar{\nu}$	2.54	1.40	4.76	3.06
data	223	26	365	61

Table 1: Events at final selection level. Cosmic $\overset{(-)}{\nu}$ with $\phi_0 = 1.44$ and $\gamma = 2.37$

mental data, is given by:

$$p(\vec{\theta}; x) = \frac{L(x; \vec{\theta})\pi(\vec{\theta})}{\int L(x; \vec{\theta})\pi(\vec{\theta})d\vec{\theta}} \tag{2}$$

with x being the experimental data, $\vec{\theta}$ a set of parameters describing the hypothesis under test, $\pi(\vec{\theta})$ the *prior* distribution and $L(x; \vec{\theta})$ the *likelihood* function, which is the joint probability of the experimental data corresponding to the the hypothesis. The maximum of the likelihood will give the best estimation of the parameters for the hypothesis.

In our case:

$$L(N; S(\gamma), B, \phi_0) = \prod_i Poisson(N_i, B_i + \phi_0 S_i(\gamma)) \tag{3}$$

where, N_i is the number of data events in bin i, S_i is the number of expected signal events for a given spectral index γ, with $\phi_0 = 1$ and B_i is the number of expected background events. The product runs over all bins of the energy estimate.

The marginalization of the posterior probability, that is to integrate out the *nuisance* parameters, gives:

$$p(\phi_0, \gamma; N) = \int L(N; S(\gamma), B, \phi_0) \cdot \pi(B_i) \cdot \pi(S_i(\gamma)) \cdot \pi(\phi_0, \gamma) \cdot \prod_i dB_i dS_i(\gamma) \tag{4}$$

The prior distributions incorporate the uncertainties of the MC estimates. Here: $\pi(B_i) = Gaussian(\mu = B_i, \sigma = \sigma_{B_i})$, $\pi(S_i(\gamma)) = Gaussian(\mu = 1, \sigma = \sigma_{S_i})$ are used, and $\pi(\phi_0, \gamma) = 1$, since no previous knowledge of ϕ_0 and γ is assumed.

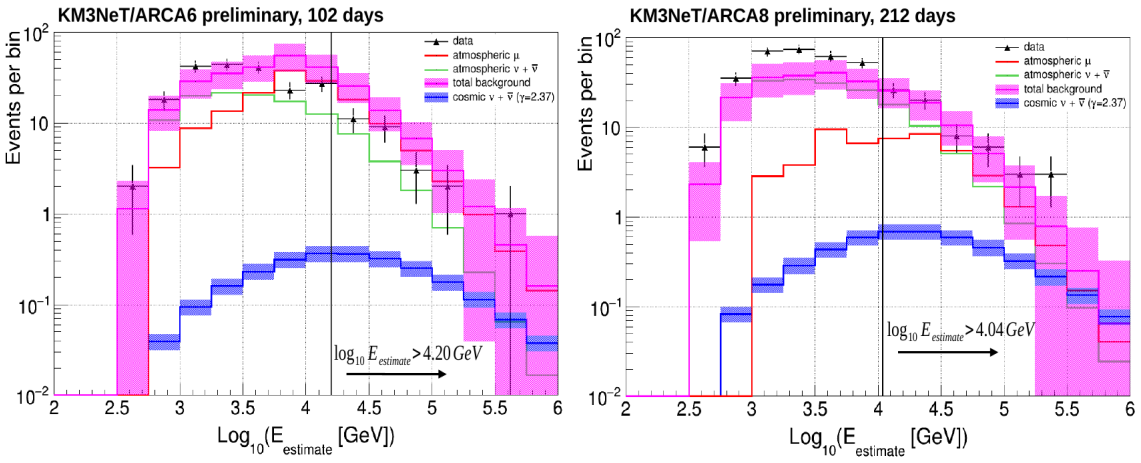

Figure 3: Distributions of the energy estimate for ARCA6 and ARCA8 after applying the BDT score cut. The total background of atmospheric neutrinos and muons (purple) and signal (blue) are shown with their total uncertainties. The vertical line in each plot shows the optimal threshold of the energy estimate.

4.2 Uncertainties

Statistical and systematic uncertainties are taken into account through the gaussian priors of eq. 4. For both the ARCA6 and ARCA8 running periods, the same uncertainties were considered. For the *signal*, an overall uncertainty of 20% for every energy bin is assumed. For the *background* the total uncertainty, for every energy bin, is given as:

$$\sigma_{B_i} = \sqrt{\sigma^2_{M_i} + \sigma^2_{A_i}} = \sqrt{\sigma^2_{stat,(M_i)} + \sigma^2_{data/mc,(M_i)} + \sigma^2_{stat,(A_i)} + \sigma^2_{simulation,(A_i)}} \tag{5}$$

since the background (B) consists of of atmospheric $\nu + \bar{\nu}$ (A) and atmospheric μ (M).

Here, $\sigma_{stat,(M_i)}$ and $\sigma_{stat,(A_i)}$ is the statistical error for atmospheric muons and atmospheric (anti)neutrinos respectively. $\sigma_{data/mc,(M_i)}$ is the systematic uncertainty for the atmospheric muon background estimation equal to 40% due to the difference between data and the expected events from MC simulation. $\sigma_{simulation,(A_i)}$ is the collective uncertainty on the atmospheric (anti)neutrino simulation, equal also to 40%. Uncertainties on the (anti)neutrino simulation come from the effect of uncertainties on the water properties, the uncertainty on the PMTs efficiency and the atmospheric (anti)neutrino flux normalization [11].

5. ARCA19/ARCA21 samples

A similar procedure, as the one described in previous sections, was followed for the ARCA19 and ARCA21 data samples. After some tests, the same *Preselection* as for ARCA6/8 periods was applied to the ARCA19/21. A special MC production dedicated to be used in machine learning (ML) techniques was made for both the ARCA19 and the ARCA21 periods. A BDT was trained on the combination of the two ML samples with the same *class 0* and *class 1* as for ARCA6/8. The model used the same hyper-parameters and similar input variables. An additional constraint based on a different way of calculating the length of the track was applied for ARCA19/21. The optimization of the BDT and the MRF procedure returned a BDT score > 0.45 and $\log E_{estimate}$ > 4.12 GeV,

and BDT score > 0.40 and $\log E_{estimate}$ > 4.36 GeV for ARCA19 and ARCA21 respectively. The same statistical analysis strategy was followed for those two periods. After applying the BDT score cut, a fit to the atmospheric muon energy distribution was performed for both periods. *No* other modifications to the MC were made (in contrast to ACA6/8). Following eq. 5, a *conservative* systematic uncertainty of 40% was applied to the atmospheric muon contribution, and also a 40% systematic uncertainty on the atmospheric (anti)neutrino simulation. A 20% total uncertainty was applied to the signal. The same binned-likelihood method was exploited for the ARCA19/21 periods and their combination with ARCA6/8.

6. Results

For the computation of the Likelihood, 8 bins for the $\log E_{estimate} \in$ [4,6] were used for each period. The spectral index was scanned in the range [1,4], and the flux normalization, ϕ_0, in [0.001,10].

By profiling the posterior (eq. 4) to specific spectral indices, the upper limits (U.L.s) to the diffuse astrophysical neutrino flux are found. In Table 2, the 90% confidence level (C.L.) U.L.s are given for our baseline $\gamma = 2.37$ and also for $\gamma = 2.0$ and 2.5 in order to compare with the values reported by ANTARES' all-flavour search for a diffuse flux with 9 years of data [12].

	ARCA6+8	ARCA19+21	ARCA6+8+19+21	ANTARES	5% quantile	95% quantile
$\gamma = 2.0$	5.11	3.13	2.09	4.0	15.07 TeV	11.71 PeV
$\gamma = 2.37$	6.92	4.68	3.06		5.88 TeV	1.73 PeV
$\gamma = 2.5$	6.76	4.94	3.12	6.8	4.43 TeV	1.03 PeV

Table 2: 90% C.L. upper limits for ARCA6+ARCA8 and ARCA19+ARCA21 periods and their combination compared with 9 years of ANTARES, computed for the central 90% energy range of the signal events. Numbers reported are $\times 10^{-18}$[GeV^{-1}cm^{-2}s^{-1}sr^{-1}] in accordance to eq. 1. Energy quantiles refer to the combined ARCA6+8+19+21 period.

The convolution of sensitivities and U.L.s for selected spectral indices in the range [2.1,2.5] in terms of energy-flux $E^2\Phi(E)$ versus the (anti)neutrino energy, calculated for the central 90% energy range of the signal events, can be seen in Figure 4.

7. Conclusions and outlook

In this work, an analysis of the full dataset collected from the first KM3NeT/ARCA configuration of appreciable volume, namely ARCA6 & ARCA8, and also of the recent configuration ARCA19 & ARCA21 was presented, focusing on the search for a 3f diffuse astrophysical neutrino flux. Calculations were performed using as a baseline the one-flavour IceCube neutrino flux with $\Phi_0 = 1.44 \cdot 10^{-18}$ and $\gamma = 2.37$ at 100 TeV normalization. An event selection was applied for all periods with a similar preselection and by considering only *upgoing* events. A BDT was used to further discriminate signal from background. The MRF procedure was applied for selecting the BDT score and the cut on the optimal energy estimate for each period. A binned likelihood method was used for the statistical analysis of the signal properties. Statistical and systematic uncertainties were taken into account. The 90% upper limits set on the cosmic neutrino flux for various spectral indices are reported, and compared with the ones obtained with 9 years of ANTARES data. The

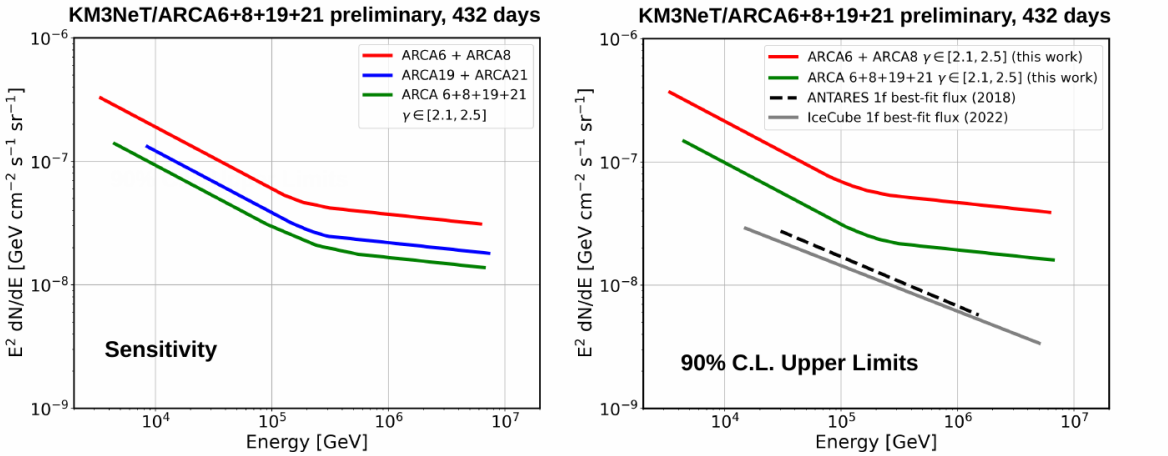

Figure 4: **(Left)** Convolution of sensitivities at 90% C.L. for selected γ in range [2.1,2.5] for ARCA6+ARCA8, ARCA19+ARCA21 and their combination, computed for the central 90% energy range of the signal events. **(Right)** Convolution of U.L.s at 90% C.L. for the same spectral indicies and energy ranges. As a comparison, IceCube's and ANTARES' 1-flavour best fit flux is drawn.

results are within expectations and demonstrate the potential of KM3NeT/ARCA for measuring a diffuse astrophysical neutrino flux.

Acknowledgements

Vasileios Tsourapis acknowledges the support of the Hellenic Foundation for Research and Innovation (HFRI) under the 3rd Call for HFRI PhD Fellowships (Fellowship Number: 5403).

References

[1] S. Adrián-Martínez et al. (KM3NeT Collaboration), 2016 J. Phys. G 43 084001
[2] The KM3NeT Collaboration, 2022 JINST 17 P07038, DOI:10.1088/1748-0221/17/07/P07038
[3] Sinopoulou A. et al. (2022), Zenodo. https://doi.org/10.5281/zenodo.6767724
[4] A. Hoecker et al., PoS A CAT 040 (2007) [physics/0703039]
[5] Honda M., Kajita T., Kasahara, K., Midorikawa, S., & Sanuki, T. 2007, PhRvD, 75, 043006
[6] Enberg, R., Reno, M. H., & Sarcevic, I. 2008, PhRvD, 78, 043005
[7] R. Abbasi et al. 2022 ApJ 928 50, DOI:10.3847/1538-4357/ac4d29
[8] Gary C. Hill, Katherine Rawlins, 2003, Astropart. Phys., 19, 393
[9] Feldman G.J., & Cousins R.D., 1998, PhRvD, 57, 3873
[10] ANTARES Collaboration, 2023, Phys. Lett. B, 841, 137951
[11] Filippini F., PoS(ICRC2023)1190
[12] A. Albert et al 2018 ApJL 853 L7, DOI:10.3847/2041-8213/aaa4f6

Full Authors List: The KM3NeT Collaboration

S. Aiello[a], A. Albert[b,bd], S. Alves Garre[c], Z. Aly[d], A. Ambrosone[f,e], F. Ameli[g], M. Andre[h], E. Androutsou[i], M. Anguita[j], L. Aphecetche[k], M. Ardid[l], S. Ardid[l], H. Atmani[m], J. Aublin[n], L. Bailly-Salins[o], Z. Bardačová[q,p], B. Baret[n], A. Bariego-Quintana[c], S. Basegmez du Pree[r], Y. Becherini[n], M. Bendahman[m,n], F. Benfenati[t,s], M. Benhassi[u,e], D. M. Benoit[v], E. Berbee[r], V. Bertin[d], S. Biagi[w], M. Boettcher[x], D. Bonanno[w], J. Boumaaza[m], M. Bouta[y], M. Bouwhuis[r], C. Bozza[z,e], R. M. Bozza[f,e], H.Brânzaş[aa], F. Bretaudeau[k], R. Bruijn[ab,r], J. Brunner[d], R. Bruno[a], E. Buis[ac,r], R. Buompane[u,e], J. Busto[d], B. Caiffi[ad], D. Calvo[c], S. Campion[g,ae], A. Capone[g,ae], F. Carenini[t,s], V. Carretero[c], T. Cartraud[n], P. Castaldi[af,s], V. Cecchini[c], S. Celli[g,ae], L. Cerisy[d], M. Chabab[ag], M. Chadolias[ah], A. Chen[ai], S. Cherubini[aj,w], T. Chiarusi[s], M. Circella[ak], R. Cocimano[w], J. A. B. Coelho[n], A. Coleiro[n], R. Coniglione[w] P. Coyle[d], A. Creusot[n], A. Cruz[al], G. Cuttone[w], R. Dallier[k], Y. Darras[ah], A. De Benedittis[e], B. De Martino[d], V. Decoene[k], R. Del Burgo[e], U. M. Di Cerbo[e], L. S. Di Mauro[w], I. Di Palma[g,ae], A. F. Díaz[j], C. Diaz[j], D. Diego-Tortosa[w], C. Distefano[w], A. Domi[ah], C. Donzaud[n], D. Dornic[d], M. Dörr[am], E. Drakopoulou[i], D. Drouhin[b,bd], R. Dvornický[q], T. Eberl[ah], E. Eckerová[q,p], A. Eddymaoui[m], T. van Eeden[r], M. Eff[n], D. van Eijk[r], I. El Bojaddaini[y], S. El Hedri[n], A. Enzenhöfer[d], G. Ferrara[w], M. D. Filipović[an], F. Filippini[t,s], D. Franciotti[w], L. A. Fusco[z,e], J. Gabriel[ao], S. Gagliardini[g], T. Gal[ah], J. García Méndez[l], A. Garcia Soto[c], C. Gatius Oliver[r], N. Geißelbrecht[ah], H. Ghaddari[y], L. Gialanella[e,u], B. K. Gibson[v], E. Giorgio[w], I. Goos[n], D. Goupilliere[o], S. R. Gozzini[c], R. Gracia[ah], K. Graf[ah], C. Guidi[ap,ad], B. Guillon[o], M. Gutiérrez[aq], H. van Haren[ar], A. Heijboer[r], A. Hekalo[am], L. Hennig[ah], J. J. Hernández-Rey[c], F. Huang[d], W. Idrissi Ibnsalih[e], G. Illuminati[s], C. W. James[al], M. de Jong[as,r], P. de Jong[ab,r], B. J. Jung[r], P. Kalaczyński[at,be], O. Kalekin[ah], U. F. Katz[ah], N. R. Khan Chowdhury[c], A. Khatun[q], G. Kistauri[av,au], C. Kopper[ah], A. Kouchner[aw,n], V. Kulikovskiy[ad], R. Kvatadze[av], M. Labalme[o], R. Lahmann[ah], G. Larosa[w], C. Lastoria[d], A. Lazo[c], S. Le Stum[d], G. Lehaut[o], E. Leonora[a], N. Lessing[c], G. Levi[t,s], M. Lindsey Clark[n], F. Longhitano[a], J. Majumdar[r], L. Malerba[ad], F. Mamedov[p], J. Mańczak[c], A. Manfreda[e], M. Marconi[ap,ad], A. Margiotta[t,s], A. Marinelli[e,f], C. Markou[i], L. Martin[k], J. A. Martínez-Mora[l], F. Marzaioli[u,e], M. Mastrodicasa[ae,g], S. Mastroianni[e], S. Miccichè[w], G. Miele[f,e], P. Migliozzi[e], E. Migneco[w], M. L. Mitsou[e], C. M. Mollo[e], L. Morales-Gallegos[u,e], C. Morley-Wong[al], A. Moussa[y], I. Mozun Mateo[ay,ax], R. Muller[r], M. R. Musone[e,u], M. Musumeci[w], L. Nauta[r], S. Navas[aq], A. Nayerhoda[ak], C. A. Nicolau[g], B. Nkosi[ai], B. Ó Fearraigh[ab,r], V. Oliviero[f,e], A. Orlando[w], E. Oukacha[n], D. Paesani[w], J. Palacios González[c], G. Papalashvili[au], V. Parisi[ap,ad], E.J. Pastor Gomez[c], A. M. Păun[aa], G. E. Păvălaş[aa], S. Peña Martínez[n], M. Perrin-Terrin[d], J. Perronnel[o], V. Pestel[ay], R. Pestes[n], P. Piattelli[w], C. Poirè[z,e], V. Popa[aa], T. Pradier[b], S. Pulvirenti[w], G. Quéméner[o], C. Quiroz[l], U. Rahaman[c], N. Randazzo[a], R. Randriatoamanana[k], S. Razzaque[az], I. C. Rea[e], D. Real[c], S. Reck[ah], G. Riccobene[w], J. Robinson[x], A. Romanov[ap,ad], A. Šaina[c], F. Salesa Greus[c], D. F. E. Samtleben[as,r], A. Sánchez Losa[c,ak], S. Sanfilippo[w], M. Sanguineti[ap,ad], C. Santonastaso[ba,e], D. Santonocito[w], P. Sapienza[w], J. Schnabel[ah], J. Schumann[ah], H. M. Schutte[x], J. Seneca[r], N. Sennan[y], B. Setter[ah], I. Sgura[ak], R. Shanidze[au], Y. Shitov[p], F. Šimkovic[q], A. Simonelli[e], A. Sinopoulou[a], M.V. Smirnov[ah], B. Spisso[e], M. Spurio[t,s], D. Stavropoulos[i], I. Štekl[p], M. Taiuti[ap,ad], Y. Tayalati[m], H. Tedjditi[ad], H. Thiersen[x], I. Tosta e Melo[a,aj], B. Trocmé[n], V. Tsourapis[i], E. Tzamariudaki[i], A. Vacheret[o], V. Valsecchi[w], V. Van Elewyck[aw,n], G. Vannoye[d], G. Vasileiadis[bb], F. Vazquez de Sola[r], C. Verilhac[n], A. Veutro[g,ae], S. Viola[w], D. Vivolo[u,e], J. Wilms[bc], E. de Wolf[ab,r], H. Yepes-Ramirez[l], G. Zarpapis[i], S. Zavatarelli[ad], A. Zegarelli[g,ae], D. Zito[w], J. D. Zornoza[c], J. Zúñiga[c], and N. Zywucka[x].

[a] INFN, Sezione di Catania, Via Santa Sofia 64, Catania, 95123 Italy
[b] Université de Strasbourg, CNRS, IPHC UMR 7178, F-67000 Strasbourg, France
[c] IFIC - Instituto de Física Corpuscular (CSIC - Universitat de València), c/Catedrático José Beltrán, 2, 46980 Paterna, Valencia, Spain
[d] Aix Marseille Univ, CNRS/IN2P3, CPPM, Marseille, France
[e] INFN, Sezione di Napoli, Complesso Universitario di Monte S. Angelo, Via Cintia ed. G, Napoli, 80126 Italy
[f] Università di Napoli "Federico II", Dip. Scienze Fisiche "E. Pancini", Complesso Universitario di Monte S. Angelo, Via Cintia ed. G, Napoli, 80126 Italy
[g] INFN, Sezione di Roma, Piazzale Aldo Moro 2, Roma, 00185 Italy
[h] Universitat Politècnica de Catalunya, Laboratori d'Aplicacions Bioacústiques, Centre Tecnològic de Vilanova i la Geltrú, Avda. Rambla Exposició, s/n, Vilanova i la Geltrú, 08800 Spain
[i] NCSR Demokritos, Institute of Nuclear and Particle Physics, Ag. Paraskevi Attikis, Athens, 15310 Greece
[j] University of Granada, Dept. of Computer Architecture and Technology/CITIC, 18071 Granada, Spain
[k] Subatech, IMT Atlantique, IN2P3-CNRS, Université de Nantes, 4 rue Alfred Kastler - La Chantrerie, Nantes, BP 20722 44307 France
[l] Universitat Politècnica de València, Instituto de Investigación para la Gestión Integrada de las Zonas Costeras, C/ Paranimf, 1, Gandia, 46730 Spain
[m] University Mohammed V in Rabat, Faculty of Sciences, 4 av. Ibn Battouta, B.P. 1014, R.P. 10000 Rabat, Morocco
[n] Université Paris Cité, CNRS, Astroparticule et Cosmologie, F-75013 Paris, France
[o] LPC CAEN, Normandie Univ, ENSICAEN, UNICAEN, CNRS/IN2P3, 6 boulevard Maréchal Juin, Caen, 14050 France
[p] Czech Technical University in Prague, Institute of Experimental and Applied Physics, Husova 240/5, Prague, 110 00 Czech Republic
[q] Comenius University in Bratislava, Department of Nuclear Physics and Biophysics, Mlynska dolina F1, Bratislava, 842 48 Slovak Republic
[r] Nikhef, National Institute for Subatomic Physics, PO Box 41882, Amsterdam, 1009 DB Netherlands
[s] INFN, Sezione di Bologna, v.le C. Berti-Pichat, 6/2, Bologna, 40127 Italy
[t] Università di Bologna, Dipartimento di Fisica e Astronomia, v.le C. Berti-Pichat, 6/2, Bologna, 40127 Italy
[u] Università degli Studi della Campania "Luigi Vanvitelli", Dipartimento di Matematica e Fisica, viale Lincoln 5, Caserta, 81100 Italy
[v] E. A. Milne Centre for Astrophysics, University of Hull, Hull, HU6 7RX, United Kingdom

[w] INFN, Laboratori Nazionali del Sud, Via S. Sofia 62, Catania, 95123 Italy
[x] North-West University, Centre for Space Research, Private Bag X6001, Potchefstroom, 2520 South Africa
[y] University Mohammed I, Faculty of Sciences, BV Mohammed VI, B.P. 717, R.P. 60000 Oujda, Morocco
[z] Università di Salerno e INFN Gruppo Collegato di Salerno, Dipartimento di Fisica, Via Giovanni Paolo II 132, Fisciano, 84084 Italy
[aa] ISS, Atomistilor 409, Măgurele, RO-077125 Romania
[ab] University of Amsterdam, Institute of Physics/IHEF, PO Box 94216, Amsterdam, 1090 GE Netherlands
[ac] TNO, Technical Sciences, PO Box 155, Delft, 2600 AD Netherlands
[ad] INFN, Sezione di Genova, Via Dodecaneso 33, Genova, 16146 Italy
[ae] Università La Sapienza, Dipartimento di Fisica, Piazzale Aldo Moro 2, Roma, 00185 Italy
[af] Università di Bologna, Dipartimento di Ingegneria dell'Energia Elettrica e dell'Informazione "Guglielmo Marconi", Via dell'Università 50, Cesena, 47521 Italia
[ag] Cadi Ayyad University, Physics Department, Faculty of Science Semlalia, Av. My Abdellah, P.O.B. 2390, Marrakech, 40000 Morocco
[ah] Friedrich-Alexander-Universität Erlangen-Nürnberg (FAU), Erlangen Centre for Astroparticle Physics, Nikolaus-Fiebiger-Straße 2, 91058 Erlangen, Germany
[ai] University of the Witwatersrand, School of Physics, Private Bag 3, Johannesburg, Wits 2050 South Africa
[aj] Università di Catania, Dipartimento di Fisica e Astronomia "Ettore Majorana", Via Santa Sofia 64, Catania, 95123 Italy
[ak] INFN, Sezione di Bari, via Orabona, 4, Bari, 70125 Italy
[al] International Centre for Radio Astronomy Research, Curtin University, Bentley, WA 6102, Australia
[am] University Würzburg, Emil-Fischer-Straße 31, Würzburg, 97074 Germany
[an] Western Sydney University, School of Computing, Engineering and Mathematics, Locked Bag 1797, Penrith, NSW 2751 Australia
[ao] IN2P3, LPC, Campus des Cézeaux 24, avenue des Landais BP 80026, Aubière Cedex, 63171 France
[ap] Università di Genova, Via Dodecaneso 33, Genova, 16146 Italy
[aq] University of Granada, Dpto. de Física Teórica y del Cosmos & C.A.F.P.E., 18071 Granada, Spain
[ar] NIOZ (Royal Netherlands Institute for Sea Research), PO Box 59, Den Burg, Texel, 1790 AB, the Netherlands
[as] Leiden University, Leiden Institute of Physics, PO Box 9504, Leiden, 2300 RA Netherlands
[at] National Centre for Nuclear Research, 02-093 Warsaw, Poland
[au] Tbilisi State University, Department of Physics, 3, Chavchavadze Ave., Tbilisi, 0179 Georgia
[av] The University of Georgia, Institute of Physics, Kostava str. 77, Tbilisi, 0171 Georgia
[aw] Institut Universitaire de France, 1 rue Descartes, Paris, 75005 France
[ax] IN2P3, 3, Rue Michel-Ange, Paris 16, 75794 France
[ay] LPC, Campus des Cézeaux 24, avenue des Landais BP 80026, Aubière Cedex, 63171 France
[az] University of Johannesburg, Department Physics, PO Box 524, Auckland Park, 2006 South Africa
[ba] Università degli Studi della Campania "Luigi Vanvitelli", CAPACITY, Laboratorio CIRCE - Dip. Di Matematica e Fisica - Viale Carlo III di Borbone 153, San Nicola La Strada, 81020 Italy
[bb] Laboratoire Univers et Particules de Montpellier, Place Eugène Bataillon - CC 72, Montpellier Cédex 05, 34095 France
[bc] Friedrich-Alexander-Universität Erlangen-Nürnberg (FAU), Remeis Sternwarte, Sternwartstraße 7, 96049 Bamberg, Germany
[bd] Université de Haute Alsace, rue des Frères Lumière, 68093 Mulhouse Cedex, France
[be] AstroCeNT, Nicolaus Copernicus Astronomical Center, Polish Academy of Sciences, Rektorska 4, Warsaw, 00-614 Poland

Acknowledgements

The authors acknowledge the financial support of the funding agencies: Agence Nationale de la Recherche (contract ANR-15-CE31-0020), Centre National de la Recherche Scientifique (CNRS), Commission Européenne (FEDER fund and Marie Curie Program), LabEx UnivEarthS (ANR-10-LABX-0023 and ANR-18-IDEX-0001), Paris Île-de-France Region, France; Shota Rustaveli National Science Foundation of Georgia (SRNSFG, FR-22-13708), Georgia; The General Secretariat of Research and Innovation (GSRI), Greece Istituto Nazionale di Fisica Nucleare (INFN), Ministero dell'Università e della Ricerca (MIUR), PRIN 2017 program (Grant NAT-NET 2017W4HA7S) Italy; Ministry of Higher Education, Scientific Research and Innovation, Morocco, and the Arab Fund for Economic and Social Development, Kuwait; Nederlandse organisatie voor Wetenschappelijk Onderzoek (NWO), the Netherlands; The National Science Centre, Poland (2021/41/N/ST2/01177); The grant "AstroCeNT: Particle Astrophysics Science and Technology Centre", carried out within the International Research Agendas programme of the Foundation for Polish Science financed by the European Union under the European Regional Development Fund; National Authority for Scientific Research (ANCS), Romania; Grants PID2021-124591NB-C41, -C42, -C43 funded by MCIN/AEI/ 10.13039/501100011033 and, as appropriate, by "ERDF A way of making Europe", by the "European Union" or by the "European Union NextGenerationEU/PRTR", Programa de Planes Complementarios I+D+I (refs. ASFAE/2022/023, ASFAE/2022/014), Programa Prometeo (PROMETEO/2020/019) and GenT (refs. CIDEGENT/2018/034, /2019/043, /2020/049. /2021/23) of the Generalitat Valenciana, Junta de Andalucía (ref. SOMM17/6104/UGR, P18-FR-5057), EU: MSC program (ref. 101025085), Programa María Zambrano (Spanish Ministry of Universities, funded by the European Union, NextGenerationEU), Spain; The European Union's Horizon 2020 Research and Innovation Programme (ChETEC-INFRA - Project no. 101008324).